Volume 1 | Number 1 | Jan 2013 | Pages 1–100

ChemComm

Chemical Communications
www.rsc.org/chemcomm

ROYAL SOCIETY OF CHEMISTRY

This is an *Accepted Manuscript*, which has been through the Royal Society of Chemistry peer review process and has been accepted for publication.

Accepted Manuscripts are published online shortly after acceptance, before technical editing, formatting and proof reading. Using this free service, authors can make their results available to the community, in citable form, before we publish the edited article. We will replace this *Accepted Manuscript* with the edited and formatted *Advance Article* as soon as it is available.

You can find more information about *Accepted Manuscripts* in the **Information for Authors**.

Please note that technical editing may introduce minor changes to the text and/or graphics, which may alter content. The journal's standard **Terms & Conditions** and the **Ethical guidelines** still apply. In no event shall the Royal Society of Chemistry be held responsible for any errors or omissions in this *Accepted Manuscript* or any consequences arising from the use of any information it contains.

www.rsc.org/chemcomm

ChemComm

COMMUNICATION

Efficient and Synergetic DNA Delivery with Pyridinium Amphiphiles – Gold Nanoparticle Composite Systems Having Different Packing Parameters

Adrian Kizewski[a], Marc A. Ilies[b,c*]

Mixtures of highly curved pyridinium-decorated Au nanoparticles and standard pyridinium cationic lipids efficiently and synergetically transfected DNA in vitro, while displaying an excellent cytotoxic profile.

Efficient delivery of nucleic acids for therapeutic purposes requires delivery systems able to compact the genetic material, maintain its structural integrity while overcoming various delivery barriers, and unload the genetic cargo to the nucleus (for DNA) or to the cytoplasm (for siRNA) of target cells/tissues.[1-4] Synthetic transfection systems based on cationic lipids and other amphiphiles (lipoplexes)[1,5,6] or cationic polymers (polyplexes)[2] provide a safer alternative to viruses but their efficiency must be improved. In this context, it was shown by us and by others that pyridinium amphiphiles are particular well suited for overcoming the hurdles of compaction/release process.[1,7-12] Extensive structure-activity relationships studies[1,7-9,13] established pyridinium lipids **SAINT-2, SPYRIT-7, Ole** and gemini surfactants **SPYRIT-68** as efficient, low toxic nucleic acid delivery systems in vitro and in vivo (Chart 1). Very recently our group proved that the properties of cationic lipids and gemini surfactants can be exploited in a synergistic manner.[14] Thus, we showed that blending 5-10% (charge equivalent) pyridinium **SPYRIT-68** into pyridinium cationic lipid **SPYRIT-7** –based lipoplexes increases the fluidity of the lipoplex bilayer, reduces the size of lipoplexes, the minimum charge ratio +/- required to fully compact the nucleic acid and significantly increases the transfection efficiency without raising the cytotoxicity of the lipoplexes.[14] These effects can be explained by the higher charge/mass ratio and lower packing parameter of pyridinium gemini surfactants as compared with corresponding lipids.[1,7,8] These properties translate into a higher fluidity and charge density of the lipoplex bilayer, properties revealed by Safinya's group to be essential for ensuring efficient internalization via endocytosis and endosomal escape, with positive effects on transfection efficiency.[15] We proved that addition of

gemini surfactants into the lipoplex enhances transfection through temporary poration of external and internal membranes, thus efficiently overcoming two major internal delivery barriers.
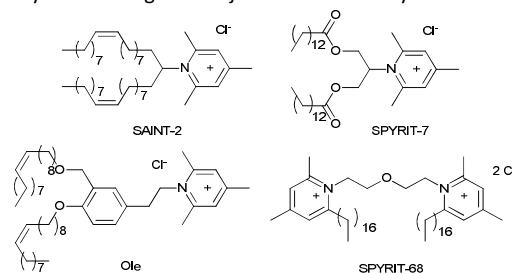

Chart 1. Representative pyridinium amphiphiles with different packing parameters used in synthetic nucleic acid delivery systems

The high charge/mass ratio and controlled interfacial curvature of gemini surfactants can be mimicked by synthetic amphiphiles chemisorbed on spherical nanoparticles of well-defined size and curvature. Particularly interesting are gold nanoparticles, due to their biocompatibility, density, and special physicochemical, optical and surface properties.[16,17] These properties recommended them for biological applications such as enzyme inhibitors and activators,[18,19] drug and gene delivery systems.[20-22] Gold compounds such as aurothioglucose, gold thiomalate, and auranofin are currently used in clinic for treatment of various forms of arthritis.[16]

Several synthetic methods are available for their generation, offering excellent control over colloidal size and surface ligands.[16] In this study we decided to employ 20 nm round Au NPs, which have a curvature comparable with typical curvatures found in hydrated self-assembled gemini surfactants with hydrophilic linkers **SPYRIT-68**.[7] This NP size was also found to be the smallest one that does not distort dramatically bilayer membranes, in related studies from our team.[23] Thus, NP size and curvature impact their interaction with the cell membrane, where a very high curvature might induce a higher cytotoxic profile through membrane poration.[24] It also controls the efficient blending with bilayer-forming cationic lipid

a.College of Science and Technology, Temple University, 1803 N Broad Street, Philadelphia, PA-19122
b.Department of Pharmaceutical Sciences and Moulder Center of Drug Discovery Research, Temple University School of Pharmacy, 3307 N Broad Street, Philadelphia, PA-19140, Email: mailies@temple.edu; Fax: +1-215-707-5620; Tel: +1-215-707-1749
*c.Temple Materials Institute, 1803 N Broad Street, Philadelphia, PA-19122*

such as **Ole** that display a cylindrical structure. From the methods available for the preparation of Au NPs we have selected the Frens method,[25] further optimized by Grabar,[26] which can generate highly homogeneous Au NPs in the desired size range with a very low polydispersity. The Au NPs generated this way have a surface decorated with citrate ligands, which are relatively easy to displace.[16,25,26]

On the other hand, the high affinity of thiols for gold drives the displacement of weak ligands such as citrate from the surface of the metal, allowing facile interfacial modification of Au NPs.[27] Thus, in order to mimic the properties of pyridinium gemini surfactants by pyridinium ligands supported by a curved Au NP, we designed and synthesized two pyridinium thiol ligands in which the two functional moieties are separated either via short (2C) or long (12C) linkers (Scheme 1). Chemisorption of fatty thiols on planar or curved gold surfaces is a well-established technique to produce self-assembled monolayers (SAMs), either planar[27] or curved.[20] The pyridinium moiety was generated in a single, high yield step via our established technology relying of the reaction of pyrylium salts with primary amines.[9,28,29] This method allowed the direct access to short mercaptoethyl pyridinium ligand **2** (as PF_6^- salt), which was converted into the more biocompatible Cl^- **3** via counterion exchange using Dowex Cl^-.[29,30] Since the Au NP surface decoration can be achieved with either thiols or disulfides, we converted the thiol **2** into the corresponding disulfide **4** via oxidation with air in DCM, followed by PF_6^- exchange to Cl^-, to yield bispyridinium disulfide **5**. The pyridinium-dodecylthiol **10** was generated from the corresponding hydroxyl derivative **6**, obtained from reaction of 12-aminododecanol with 2,4,6-trimethylpyrylium salt **1**. The hydroxyl group of **6** was converted into bromide **7** via CBr_4/PPh_3 in DCM, which was subsequently reacted with potassium thioacetate in acetone to yield the corresponding pyridinium-dodecylthioacetate **8**. The counterion of **8** was changed to Cl^- via Dowex Cl^- yielding **9**, which was transformed into the desired pyridinium-dodecylthiol **10** (as Cl^-) with aqueous HCl under inert atmosphere. The disulfide **11** was also prepared via oxidation of **10** in DCM solution with air (Scheme 1, ESI).

The direct decoration of Au NP with pyridinium mercapto derivatives **2**-**5**, **10**, **11** failed, irrespective of chain length or oxidation state of the thiol (SH or disulfide), due to fast nanoparticle aggregation. This was probably caused by the charge reversal on the Au surface upon decoration with positively charged mercapto ligands. During this process the nanoparticle surface potential shifts
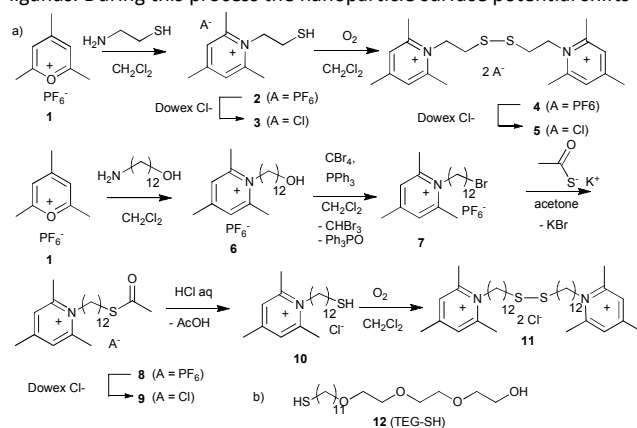
Scheme 1. a) Synthesis of pyridinium thiol and disulfide ligands for Au NP decoration, having either short (2C) or long (12C) linkers; (b) structure of HS-TEG 12 used in conjunction with pyridinium thiols in the generation of Au nanoparticles used in this study.

from negative to positive passing through a value of zero, where electrostatic repulsion is no longer present and particles can rapidly coalesce and precipitate.[31,32]

In order to sterically stabilize the Au NPs during the surface charge reversal we selected the amphiphilic triethyleneglycol mercaptan TEG-SH **12**[27] due to its amphiphilicity/wettability, excellent biocompatibility and cost. We successfully tested **12** for the surface decoration of Au NPs and we validated the stability of the resulting nanosystem. Displacement of citrate ligands by thiol **12** generated, as expected, a small increase in hydrodynamic radius of the decorated Au NP (from 21 to 25 nm) due to undecenyltriethyleneglycol-based corona, while the zeta potential remained almost unchanged (about – 8 mV, see ESI). Consequently, we performed the surface charge reversal of Au NPs by treating the citrate-decorated NPs with a blend of TEG-SH **12** with pyridinium mercapto derivatives **2**-**5**, **10**, or **11**. Systematic assessment of different thiol/**12** or disulfide/**12** combinations revealed the importance of size match between the mercapto derivatives when performing the ligand exchange of Au NP surface. Only blends of TEG-SH **12** with either pyridinium thiol **10** or with pyridinium disulfide **11** generated stable, positively charged Au NPs (Figure 1).

The short mercaptans **2**-**5** failed to stabilize the AuNPs after ligand exchange despite the presence of **12**, and coalescence of resulted NPs occurred in short time. Consequently, we focused our ligand exchange efforts on blends of TEG-SH **12** with pyridinium thiol Py-SH **10**. Optimum ligand exchange performance and stability profile of resulting Py-SH/TEG-SH Au NPs were obtained using a molar ratio of thiols **12**/**10** of 3/1. These pyridinium-decorated Au NPs (**Py-Au NPs**) had a hydrodynamic size of about 27 nm and a zeta potential of about + 30 mV after washing all released/unattached ligands. Lack of aggregation was confirmed by the color of the gold colloid, by the surface plasmon spectrum, and
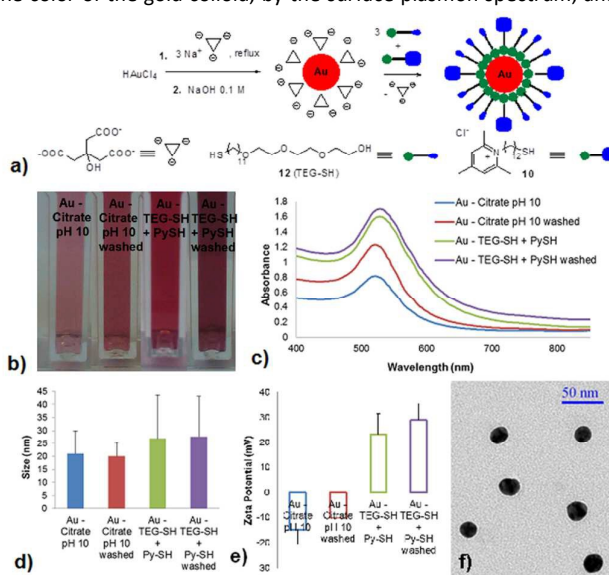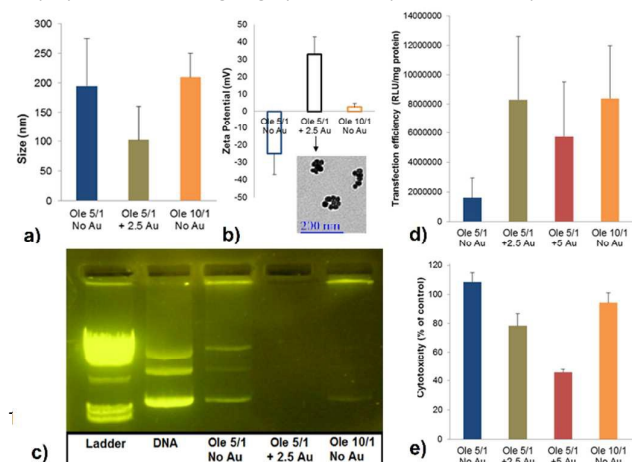
by TEM (Figure 1).

Figure 1. Synthesis and characterization of pyridinium-decorated Au nanoparticles: schematic representation of the synthesis and functionalization process (a) and physicochemical characterization throughout the stages of nanoparticle processing via color (b), surface plasmon spectrum (c), size (d), zeta potential (e) and TEM (f). See text and ESI for details.

We used these positively charged **Py-Au NPs** in subsequent DNA compaction, transfer and delivery (transfection) experiments in conjunction with the pyridinium cationic lipid **Ole** (Chart 1) optimized by our group and transfection-efficient against many cell lines.[13]

Through a combination of dynamic light scattering, zeta potential and electrophoretic mobility experiments we showed that **Ole** alone was able to fully compact plasmid DNA at a lipid/DNA charge ratio of 10, and generate lipoplexes about 200 nm in diameter, with a slightly positive (+ 4 mV) zeta potential (Figure 2a-c). A lipid/DNA charge ratio of 5 was insufficient to compact the plasmid DNA, as shown by electrophoretic mobility of resulted complexes (Figure 2c). However, adding only 2.5 equivalents of additional positive charge via blending **Py-Au NPs** in the **Ole**/DNA formulation ("Ole 5/1 + 2.5 Au") fully compacted the DNA (Figure 2c and Supplemental Figure 1, with the DNA complex of purple color due to incorporation of **Py-Au NPs**).

Interestingly, the size of the hybrid lipoplexes *decreased* to about 150 nm and their zeta potential *increased* to about + 35 mV, despite the (lower) amphiphile/DNA charge ratio of 7.5. These properties revealed the synergistic compaction effect of **Py-Au NPs** and **Ole** that allows the reduction of charge ratio while providing a better compaction of plasmid DNA (Figure 2a, 2b, with **Py-Au NPs** clearly visible in the lipoplex structure). Moreover, transfection efficiency of these hybrid lipoplexes on NCI-H23 lung cancer cell line (at charge ratio of 7.5) was found to be similar to the efficiency of **Ole** lipoplexes having a lipid/DNA charge ratio of 10, and much higher than **Ole** lipoplexes formulated at a lipid/DNA charge ratio of 5 (Figure 2d). Blending more **Py-Au NPs** in the **Ole**-based lipoplexes, for a total lipid/DNA charge ratio of 10, with 5 charge equivalents from **Ole** and 5 charge equivalents from **Py-Au NPs**, decreased the transfection efficiency and increased cytotoxicity of resulted DNA hybrid complexes. A similar effect was observed when blending (curved) pyridinium gemini surfactants **SPYRIT-68** (Chart 1) into cationic lipid-based lipoplexes,[14] reflecting a limited demand for a curved amphiphile in the lipoplex. One can consider that compaction of supercoiled plasmids involves regions of high curvature of backbone, easier to accommodate by blends of amphiphiles containing highly curved species as compared with simple lipid-only mixtures

Figure 2. Synergistic effect of DNA co-delivery by Py-Au NPs ("Au") and pyridinium cationic lipid Ole: lipoplex size (a), zeta potential (b), electrophoretic mobility (c), transfection efficiency (d) and cytotoxicity (e) on NCI-H23 lung cancer cell line.
(compare lanes 4 and 5 in Figure 2c).

The cytotoxicity of the hybrid complexes ("Ole 5/1 + 2.5 Au") was slightly higher than the **Ole**-only based lipoplexes and increased when incorporating more **Py-Au NPs** ("Ole 5/1 + 5 Au", Figure 2e). This effect also mirrored the behavior of pyridinium lipid/gemini surfactant blends.[14] In that case we could efficiently reduce the toxicity of the formulation, as well as the amount of cationic amphiphiles needed for full DNA compaction by adding co-lipids such as DOPE or cholesterol in the lipoplex formulations. Co-lipids can finely tune the packing parameter of the amphiphile blend and enhance the fluidity of the assembly and the hydrophobic effect, thus ensuring better compaction and delivery of DNA.[1,7,8]

Therefore we subsequently investigated the effect of DOPE on transfection efficiency of **Ole**-based lipoplexes and **Ole/Py-Au NPs** hybrid DNA complexes (at different compositions). We assessed the physicochemical parameters of the complexes in parallel (Figure 3). DNA complexes generated only from **Py-Au NPs** (at amphiphile/DNA charge ratios of 1 and 2, "1Au" and "2Au") and from standard transfection system Lipofectamine® were included as reference.

Data from Figure 3 revealed that **Ole**/DOPE (1/1 molar ratio) – based lipoplexes formulated at a cationic lipid/DNA charge ratio of 1 were relatively large, polydispersed and almost neutral in terms of zeta potential. As a consequence of the suboptimal physicochemical parameters, their transfection efficiency was very low. Increasing the cationic lipid/DNA charge ratio to 3 improved these physicochemical parameters, transfection efficiency and cytotoxic profile (Figure 3a, b). The biological properties of these lipoplexes were superior to the ones displayed by DNA complexes generated from **Py-Au NPs**, irrespective of the charge ratio used ("1Au" and "2Au"), also surpassing Lipofectamine-based lipoplexes (Figure 3b).
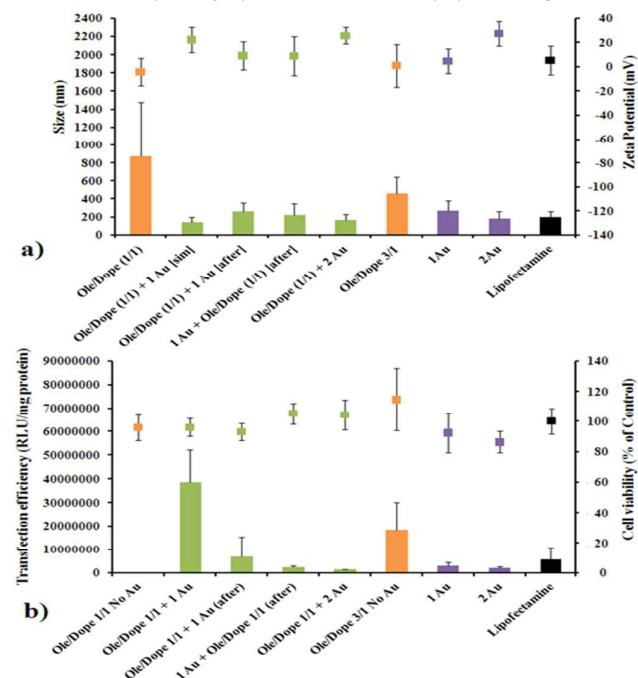
COMMUNICATION

Figure 3. Transfection efficiency and cytotoxicity of Au nanocomposite lipoplexes revealing the synergistic effect of Py-Au NPs ("Au"), pyridinium cationic lipid Ole and colipid DOPE on DNA delivery in NCI-H23 cell line.

However, hybrid **Ole**/DOPE/**Py-Au NPs** DNA complexes having an **Ole**/DOPE 1/1 molar ratio and a total amphiphile/DNA charge ratio of 2, blended together at the same time with DNA (1 charge equivalent from **Ole** and 1 charge equivalent from **Py-Au NPs**, − "Ole/Dope (1/1) + 1 Au [sim]") displayed *smaller* (~175 nm) and *more positively charged* (~ + 20 mV) lipoplexes. These hybrid DNA complexes showed a transfection efficiency superior to conventional **Ole**/Dope (1/1) lipoplexes made at a (higher) amphiphile to DNA charge ratio of 3, with an excellent cytotoxic profile, and greatly surpassing Lipofectamine-based lipoplexes. Increasing the amount of **Py-Au NPs** in the mix ("Ole/Dope (1/1) + 2 Au") had a negative effect on physicochemical and biological properties (Figure 3).

Synergetic action towards DNA compaction elicited by pyridinium cationic lipid **Ole**, colipid DOPE and **Py-Au NPs** was further proved when the plasmid DNA was treated the **Ole**/DOPE (1/1), followed by Py-Au NPs ("Ole/Dope (1/1) + 1 Au [after]") or vice-versa, with **Py-Au NPs**, followed by **Ole**/DOPE (1/1) ("1 Au + Ole/Dope (1/1) [after]", Figure 3). These DNA complexes were inferior in both physicochemical and biological properties to the complexes formed by simultaneous addition of **Ole**/DOPE (1/1) and **Py-Au NPs** to DNA.

The superior physicochemical and biological properties of these hybrid nanosystems based on pyridinium amphiphiles constitute another direct proof of synergetic action towards nucleic acid delivery of different classes of amphiphiles with controlled packing parameters,[1,7,8] across different types of colloidal materials.[16,17,33-35]

Acknowledgements

Notes and references

1. B. Draghici and M. A. Ilies, *J. Med. Chem.*, 2015, **58**, 4091.
2. H. Yin, R. L. Kanasty, A. A. Eltoukhy, A. J. Vegas, J. R. Dorkin and D. G. Anderson, *Nat. Rev. Genet.*, 2014, **15**, 541.
3. W. Li and F. C. Szoka, Jr., *Pharm. Res.*, 2007, **24**, 438.
4. T. R. Pearce, K. Shroff and E. Kokkoli, *Adv. Mater.*, 2012, **24**, 3803.
5. T. Montier, T. Benvegnu, P. A. Jaffres, J. J. Yaouanc and P. Lehn, *Curr. Gene Ther.*, 2008, **8**, 296.
6. S. Bhattacharya and A. Bajaj, *Chem. Commun*, 2009, 4632.
7. V. D. Sharma and M. A. Ilies, *Med. Res. Rev.*, 2014, **34**, 1.
8. M. A. Ilies, T. V. Sommers, L. C. He, A. Kizewski and V. D. Sharma, in *Amphiphiles: Molecular Assembly and Applications*, ed. R. Nagarajan, ACS Symposium Series, Washington, DC, 2011, Ch. 2, pp. 23-38.
9. M. A. Ilies, W. A. Seitz, B. H. Johnson, E. L. Ezell, A. L. Miller, E. B. Thompson and A. T. Balaban, *J. Med. Chem.*, 2006, **49**, 3872.
10. Arthur A. P. Meekel, A. Wagenaar, J. Šmisterová, Jessica E. Kroeze, P. Haadsma, B. Bosgraaf, Marc C. A. Stuart, A. Brisson,

11. Marcel H. J. Ruiters, D. Hoekstra and Jan B. F. N. Engberts, *Eur. J. Org. Chem.*, 2000, 665.
11. I. van der Woude, A. Wagenaar, A. A. Meekel, M. B. ter Beest, M. H. Ruiters, J. B. Engberts and D. Hoekstra, *Proc. Natl. Acad. Sci. U S A*, 1997, **94**, 1160.
12. S. S. Le Corre, N. Belmadi, M. Berchel, T. Le Gall, J. P. Haelters, P. Lehn, T. Montier and P. A. Jaffres, *Org. Biomol. Chem.*, 2015, **13**, 1122.
13. S. Savarala, E. Brailoiu, S. L. Wunder and M. A. Ilies, *Biomacromolecules*, 2013, **14**, 2750.
14. V. D. Sharma, J. Lees, N. E. Hoffman, E. Brailoiu, M. Madesh, S. L. Wunder and M. A. Ilies, *Mol. Pharm.*, 2014, **11**, 545.
15. A. J. Lin, N. L. Slack, A. Ahmad, C. X. George, C. E. Samuel and C. R. Safinya, *Biophys. J.*, 2003, **84**, 3307.
16. E. C. Dreaden, A. M. Alkilany, X. Huang, C. J. Murphy and M. A. El-Sayed, *Chem. Soc. Rev.*, 2012, **41**, 2740.
17. R. A. Sperling, P. Rivera Gil, F. Zhang, M. Zanella and W. J. Parak, *Chem. Soc. Rev.*, 2008, **37**, 1896.
18. M. Stiti, A. Cecchi, M. Rami, M. Abdaoui, V. Barragan-Montero, A. Scozzafava, Y. Guari, J. Y. Winum and C. T. Supuran, *J. Am. Chem. Soc.*, 2008, **130**, 16130.
19. M. C. Saada, J. L. Montero, D. Vullo, A. Scozzafava, J. Y. Winum and C. T. Supuran, *J. Med. Chem.*, 2011, **54**, 1170.
20. Y. Ding, Z. Jiang, K. Saha, C. S. Kim, S. T. Kim, R. F. Landis and V. M. Rotello, *Mol. Ther.*, 2014, **22**, 1075.
21. P. Ghosh, G. Han, M. De, C. K. Kim and V. M. Rotello, *Adv. Drug Deliv. Rev.*, 2008, **60**, 1307.
22. A. Fernandez-Barbero, I. J. Suarez, B. Sierra-Martín, A. Fernandez-Nieves, F. Javier de las Nieves, M. Marquez, J. Rubio-Retama, E. Lopez-Cabarcos, *Adv. Coll. Interface Sci.* 2009, **147–148**, 88.
23. S. Savarala, S. Ahmed, M. A. Ilies and S. L. Wunder, *Langmuir*, 2010, **26**, 12081.
24. L. Shang, K. Nienhaus and G. U. Nienhaus *J. Nanobiotechnol.* 2014, **12**, 1.
25. G. Frens, *Nature-Phys. Sci.*, 1973, **241**, 20.
26. K. C. Grabar, R. G. Freeman, M. B. Hommer and M. J. Natan, *Anal. Chem.*, 1995, **67**, 735.
27. J. C. Love, L. A. Estroff, J. K. Kriebel, R. G. Nuzzo and G. M. Whitesides, *Chem. Rev.*, 2005, **105**, 1103.
28. M. A. Ilies, W. A. Seitz, M. T. Caproiu, M. Wentz, R. E. Garfield and A. T. Balaban, *Eur. J. Org. Chem.*, 2003, 2645.
29. M. A. Ilies, W. A. Seitz, I. Ghiviriga, B. H. Johnson, A. Miller, E. B. Thompson and A. T. Balaban, *J. Med. Chem.*, 2004, **47**, 3744.
30. V. D. Sharma, E. O. Aifuwa, P. A. Heiney and M. A. Ilies, *Biomaterials*, 2013, **34**, 6906.
31. S. Savarala, F. Monson, M. A. Ilies and S. L. Wunder, *Langmuir*, 2011, **27**, 5850.
32. S. Savarala, S. Ahmed, M. A. Ilies and S. L. Wunder, *ACS Nano*, 2011, **5**, 2619.
33. J. O. Radler, I. Koltover, T. Salditt and C. R. Safinya, *Science*, 1997, **275**, 810.
34. I. Koltover, T. Salditt, J. O. Radler and C. R. Safinya, *Science*, 1998, **281**, 78.
35. E. Mahon, T. Aastrup and M. Barboiu, *Top. Curr. Chem.*, 2012, **322**, 139.